Biogeosciences

Physiological and biochemical responses of *Emiliania huxleyi* to ocean acidification and warming are modulated by UV radiation

Shanying Tong[1,3], **David A. Hutchins**[2], **and Kunshan Gao**[1]

[1]State Key Laboratory of Marine Environmental Science, Xiamen University, Xiamen, China
[2]Department of Biological Sciences, University of Southern California, Los Angeles, California, USA
[3]College of Life Science, Ludong University, Yantai, China

Correspondence: Kunshan Gao (ksgao@xmu.edu.cn)

Abstract. Marine phytoplankton such as bloom-forming, calcite-producing coccolithophores, are naturally exposed to solar ultraviolet radiation (UVR, 280–400 nm) in the ocean's upper mixed layers. Nevertheless, the effects of increasing carbon dioxide (CO_2)-induced ocean acidification and warming have rarely been investigated in the presence of UVR. We examined calcification and photosynthetic carbon fixation performance in the most cosmopolitan coccolithophorid, *Emiliania huxleyi*, grown under high (1000 µatm, HC; pH_T: 7.70) and low (400 µatm, LC; pH_T: 8.02) CO_2 levels, at 15 °C, 20 °C and 24 °C with or without UVR. The HC treatment did not affect photosynthetic carbon fixation at 15 °C, but significantly enhanced it with increasing temperature. Exposure to UVR inhibited photosynthesis, with higher inhibition by UVA (320–395 nm) than UVB (295–320 nm), except in the HC and 24 °C-grown cells, in which UVB caused more inhibition than UVA. A reduced thickness of the coccolith layer in the HC-grown cells appeared to be responsible for the UV-induced inhibition, and an increased repair rate of UVA-derived damage in the HC–high-temperature grown cells could be responsible for lowered UVA-induced inhibition. While calcification was reduced with elevated CO_2 concentration, exposure to UVB or UVA affected the process differentially, with the former inhibiting it and the latter enhancing it. UVA-induced stimulation of calcification was higher in the HC-grown cells at 15 and 20 °C, whereas at 24 °C observed enhancement was not significant. The calcification to photosynthesis ratio (Cal / Pho ratio) was lower in the HC treatment, and increasing temperature also lowered the value. However, at 20 and 24 °C, exposure to UVR significantly increased the Cal / Pho ratio, especially in HC-grown cells, by up to 100 %. This implies that UVR can counteract the negative effects of the "greenhouse" treatment on the Cal / Pho ratio; hence, UVR may be a key stressor when considering the impacts of future greenhouse conditions on *E. huxleyi*.

1 Introduction

Coccolithophores are a group of calcifying unicellular phytoplankton within the Prymnesiophyceae (Paasche, 2002). They are an ecologically and biogeochemically prominent marine phytoplankton functional group, and contribute to carbon dioxide (CO_2) sinks and sources by performing both photosynthesis and calcification, respectively (Raitsos et al., 2006; Raven and Crawfurd, 2012). Although the ballasting of photosynthetic products by coccoliths helps to efficiently transport carbon from the photic zone, the calcification process is a net source of CO_2 to the environment (Rost and Riebesell, 2004; Gattuso et al., 1996). Therefore, the ratio of photosynthesis to calcification determines their net contribution to CO_2 uptake or release. Consequently, investigating changes in these two processes under varying environmental conditions is a key to our understanding of their biogeochemical roles under ocean global change. Calcification and photosynthesis of coccolithophores are influenced by many factors, including nutrients, light availability, and CO_2, as well as temperature and ultraviolet radiation (UVR) (Riebesell et al., 2017; Tong et al., 2016; Feng et al., 2008).

The rising atmospheric CO_2 concentration due to human activities causes greenhouse warming of the atmosphere and ocean, and the dissolution of this anthropogenic CO_2 into

the surface ocean reduces the pH of seawater in a process known as ocean acidification (OA). Previous studies have predicted that ongoing OA will decrease the pH by 0.40 units in pelagic waters (Gattuso et al., 2015) and by 0.45 units in coastal waters (Cai et al., 2011) by the end of this century under the business-as-usual CO_2 emissions scenario. Conversely, increased atmospheric CO_2, along with other greenhouse gases, will warm the Earth's surface by 2.5–6.4 °C by the year 2100 (Alexiadis, 2007), while the surface ocean temperature is projected to rise by 2–3 °C (Stocker et al., 2014). Most previous work has indicated that warming enhances stratification (Capotondi et al., 2012), although this has recently been disputed (Somavilla et al., 2017). Assuming that ocean warming is shoaling the depth of the upper mixed layer (UML), this would affect the integrated levels of photosynthetically active radiation (PAR) and UVR to which phytoplankton cells within the UML are exposed (Häder and Gao, 2015). Regardless, increasing concentrations of CO_2 and other greenhouse gases will also begin to play an ever-increasing role in determining levels of cloud cover and stratospheric ozone, thus affecting the amount of UVR reaching ocean surface (Williamson et al., 2014).

All of these ocean global changes may have individual and/or interactive effects on the physiology of marine primary producers (Hutchins and Fu, 2017; Gao et al., 2012). OA usually decreases the calcification of *E. huxleyi*, although corresponding $p\text{CO}_2$ increases can enhance photosynthesis or growth at the same time (Riebesell et al., 2017, 2000). Under nutrient replete conditions, increased light levels appear to counteract the negative impacts of OA on the calcification of *E. huxleyi* (Jin et al., 2017). The calcified coccoliths are thought to play roles in protection against grazing pressure, viral and bacterial attack (Monteiro et al., 2016), and can also help protect cells from UV radiation (Gao et al., 2009). Early experiments on *E. huxleyi* strain BT-6 showed that cells had a complete covering of coccoliths at 12.5–23 °C, but at 26.5 °C, 30 % of the cells had an incomplete covering (Paasche, 1968). Similarly, Langer et al. (2009) saw an increased occurrence of malformed coccoliths in *E. huxleyi* RCC 1238 at 25 °C compared with those grown at 20 and 10 °C. A recent study showed that increased temperature aggravates the impacts of OA on *E. huxleyi* morphology (Milner et al., 2016).

Increasing levels of PAR or temperature and changes in UVR and nutrient availability may interact with each other to cause additive, antagonistic or synergistic effects for coccolithophores. Nevertheless, most previous studies have been carried out under PAR only conditions, with UVR or fluctuating solar radiation not being considered. However, UVR cannot be ignored when examining the effects of environmental changes on marine phytoplankton that are found in the upper half of the euphotic zone, as UV irradiance can penetrate as deep as 80 m in pelagic waters (Tedetti et al., 2007). Excessive solar UV-B and UV-A can damage DNA and interfere with many cellular biochemical processes (Häder et al.,

2014). Conversely, moderate levels of UVA can enhance photosynthetic carbon fixation of phytoplankton assemblages (Gao et al., 2007; Helbling et al., 2003). As for UVR effects on coccolithophore calcification, recent studies have demonstrated that the outer coccoliths of *E. huxleyi* can effectively shield the cells from a certain percentage of UVR radiation (Xu et al., 2016). Nevertheless, the transmitted energy still causes a significant inhibition of calcification, as well as photosynthesis (Gao et al., 2009). The exposure of *E. huxleyi* to solar UV radiation has been found to decrease its growth rate, but increase its production of coccoliths per cell (Guan and Gao, 2009).

As exposure to solar UV radiation can influence cytoplasmic redox activities (Wu et al., 2010), and inhibit or enhance physiological performances at different levels of UVR, we hypothesized that the effects of OA and warming on coccolithophores would be different with and without the presence of UVR. To test our hypothesis, in this study we examined the responses of *E. huxleyi* photosynthesis and calcification to OA with or without UVR at three temperature levels.

2   Materials and methods

2.1   Experimental setup

The experiments used *Emiliania huxleyi* strain PML B92/11, originally isolated from the field station of the University of Bergen, Norway (Raunefjorden; 60°18′ N, 05°15′ E). To first test interactions between OA and temperature, thermal reaction curves were obtained by growing the cultures at 15, 20, 22, 24 and 27 °C in artificial seawater pre-equilibrated with elevated (1000 µatm, HC) or ambient (400 µatm, LC) atmospheric CO_2 concentrations. Triplicate experimental cultures were maintained without aeration under PAR (cool-white fluorescent lamps) of 190 µmol m^{-2} s^{-1} with a 12/12 light / dark cycle. The culture medium was enriched with 100 µmol L^{-1} nitrate and 10 µmol L^{-1} orthophosphate, and vitamins and trace metals were added according to the Aquil recipe (Sunda et al., 2005). The maximum cell concentration in all treatments was kept below 5×10^4 cells mL^{-1} in order to maintain stable carbonate chemistry (pH variation < 0.04). After the cells were grown in each treatment for about 10 generations, the growth rates were determined. The thermal reaction norms were then plotted for HC- and LC-grown cells according to the following equation:

$$f(T) = ae^{bT}\left[1 - \left(\frac{T-z}{w/2}\right)^2\right],\qquad(1)$$

where w is the temperature niche width, z is the midpoint of the growth curve, and b and a jointly determine the overall steepness, height and skewness of the curves (Thomas et al., 2012; Norberg, 2004). The optimum temperature for growth (T_{opt}) was estimated from the fitted curve by numerical optimization.

Based on T_{opt} from the thermal curve, 15, 20 and 24 °C were selected to grow the cells for another 10 generations. The rationale for choosing these temperatures is that 15 and 20 °C are below and close to the optimal growth temperature, respectively, while 24 °C is above it. To investigate how the cells responded to these three different temperature levels and two different pCO_2 levels in the presence of transient UV irradiance exposures such as those that might be encountered by cells in a dynamic mixed layer, they were then exposed to the different radiation treatments for 3 h before photosynthesis and calcification parameters were measured (Sect. 2.2.3).

2.2 Measurements and analysis

2.2.1 Growth rates

The specific growth rates (μ) were determined from cell counts performed using a Z2 Coulter counter (Beckman, Buckinghamshire, UK), calculated using the following equation: $\mu = (\ln C_1 - \ln C_0)/(t_1 - t_0)$, where t_0 and t_1 were the respective times of inoculation and sampling, $t_1 - t_0$ was the interval between inoculation and sampling, and C_0 and C_1 were the cell concentrations at time t_0 and t_1.

2.2.2 Particulate organic carbon (POC), particulate organic nitrogen (PON) and particulate inorganic nitrogen (PIC) analysis and estimation of inner coccosphere volume

After cells were cultured at 15, 20 and 24 °C for another 10 generations, duplicate samples (200 mL) taken in the middle of the light period were filtered onto 25 mm precombusted (450 °C for 6 h) Whatman GF/F filters and stored at −20 °C. For analysis, one of the duplicate filters for each treatment was fumed over HCl for 12 h to remove inorganic carbon and then dried overnight at 60 °C; the other filters were dried overnight at 60 °C directly. All the filters were then packed in tin cups and analyzed on a Perkin Elmer 2400 Series II CHNS/O analyzer. PIC was determined by the difference between TPC (total particulate carbon) and POC. The production rates of POC or PIC were calculated as $P =$ cellular POC or PIC content (pg cell^{-1}) × specific growth rate μ (d^{-1}).

The inner coccosphere (protoplast) volume (V_{cell}) were calculated according to the following equation:

$$\frac{\text{POC}\,[\text{pg}]}{\text{cell}} = a \times V_{cell}^{b}, \tag{2}$$

where a (0.216 in this case) and b (0.939 in this case) are constants which vary depending on the species investigated (Menden-Deuer and Lessard, 2000).

2.2.3 Radiation treatment and determination of calcification and photosynthetic rates

Right before the samples for elemental analysis were taken, the cells acclimated to each temperature and pCO_2 level were dispensed into 100 mL quartz tubes (volume 90 mL) and inoculated with 5 µCi (0.185 MBq) of labeled sodium bicarbonate (ICN Radiochemicals). The quartz tubes ($n = 3$) were then exposed to a solar simulator with PAR, UVA and UVB irradiance levels of 42 W m^{-2} (190 µmol m^{-2} s^{-1}), 13.5 W m^{-2} and 0.81 W m^{-2}, respectively. The radiation intensity was measured using a three channel irradiation apparatus (PMA2100, Solar Light). The PAR used was equivalent to the mean light level in the upper mixed layer (UML) based on time series station (19° N, 118.5° E) measurements in the South China Sea (Chen et al., 2006). The ratios of both UVA and UVB to PAR emitted by the solar simulator were about 30 % higher than those of the sunlight reaching the sea surface. The following three radiation treatments were realized: PAR + UVA + UVB (PAB), quartz tubes covered with 295 nm cutoff film (Ultraphan, Digefra), so that the cells were exposed to irradiances above 295 nm; PAR + UVA (PA), covered with 320 nm cutoff film (Montagefolie, Folex), with the cells exposed to irradiances above 320 nm; and PAR (P), covered with 395 nm cutoff film (Ultraphan UV Opak, Digefra), so that the cells received irradiances above 395 nm. The temperatures were controlled using a cooling circulator (CAP-3000, Rikakikai, Japan). The exposure duration lasted for 3 h, and each treatment had three replicates for the incubations. This short exposure period under the solar simulator can mimic the mixing of cells to the surface or the reappearance of sunlight after cloudiness, both of which occur frequently in nature.

The samples collected from each treatment were immediately filtered onto Whatman GF/F filters (25 mm), rinsed with unlabeled medium and put into 20 mL scintillation vials. One filter from each tube was fumed over HCl overnight to remove the coccolith coverage, and then dried at 45 °C for 4 h to estimate the photosynthetic carbon fixation rate, while the other filters were dried directly to estimate the total carbon fixation rate. A 3.5 mL scintillation cocktail (Perkin Elmer) was added to the vials, and all of the filters were counted using a liquid scintillation counter (LS 6500 Multi-Purpose Scintillation Counter, Beckman Counter, USA). The rate of calcification was determined as the difference between the total and photosynthetic carbon fixation rate. The inhibition of calcification and photosynthesis due to UVA, UVR or UVB was calculated as follows:

$$\text{Inh}_{\text{UVA}} = (R_{\text{P}} - R_{\text{PA}})/(R_{\text{P}}) \times 100\,\%$$
$$\text{Inh}_{\text{UVR}} = (R_{\text{P}} - R_{\text{PAB}})/(R_{\text{P}}) \times 100\,\%$$
$$\text{Inh}_{\text{UVB}} = (R_{\text{PA}} - R_{\text{PAB}})/(R_{\text{P}}) \times 100\,\% = \text{Inh}_{\text{UVR}} - \text{Inh}_{\text{UVA}},$$
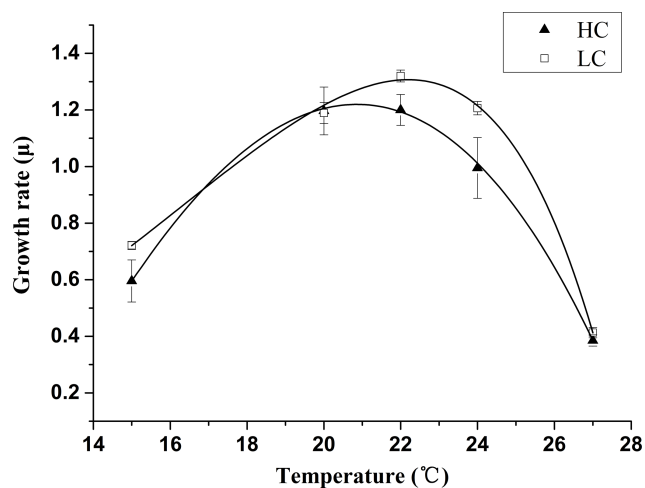
Figure 1. Thermal reaction norms of *E. huxleyi* grown in 400 µatm (LC) and 1000 µatm (HC) CO_2 concentrations. The corresponding R^2 values are 0.996 (LC) and 0.999 (HC), respectively. The values are the means, and the error bars are standard deviations for triplicate cultures for each treatment.

Figure 2. Specific growth rate of *E. huxleyi* grown in 400 µatm (LC) and 1000 µatm (HC) CO_2 concentrations at 15, 20 and 24 °C, respectively. The different letters above the bars indicate significant differences among the treatments ($p < 0.05$). The values are the means, and the error bars are standard deviations for triplicate cultures for each treatment.

where R_P, R_{PA} and R_{PAB} represented the rate of calcification or photosynthesis under PAR, PAR + UVA and PAR + UVA + UVB, respectively.

2.2.4 Estimation of carbonate chemistry

The pH of the seawater was measured using a pH meter (Benchtop pH510, Oakton) that was calibrated with standard NBS (National Bureau of Standards) buffer. The CO_2 concentration of the aeration was monitored with a CO_2 meter (Vaisala, GM70) with variations < 4 %. The cell concentrations of all cultures were maintained below 5×10^4 cells mL^{-1} to make sure that pH variations were < 0.04 units (Table 1). Other seawater carbonate system parameters were calculated with the CO2SYS software using the known parameters of pCO$_2$, salinity, pH, temperature and nutrient concentrations (Lewis et al., 1998). The carbonic acid dissociation equilibrium constants K_1 and K_2 were determined according to Roy et al. (1993) and that for boric acid was taken from Dickson (1990).

2.2.5 Data analysis

Before parametric tests were performed, data were tested for homogeneity of variance and normality. Two-way or three-way analysis of variance (ANOVA) tests were used to establish differences among the treatments. Then post hoc multiple comparisons were used to determine significant differences between temperature, CO_2 or UV treatments. Significance levels were set at $p < 0.05$.
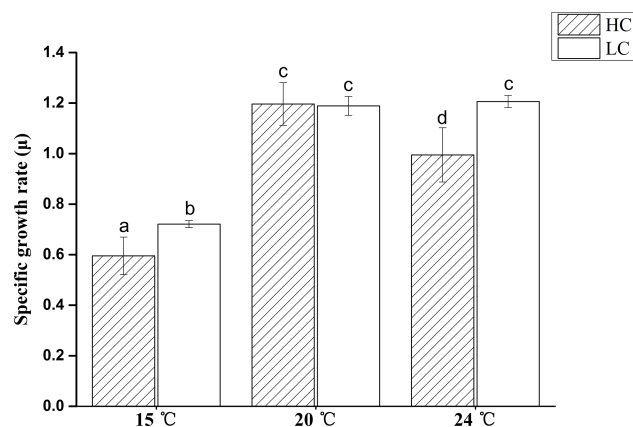
3 Results

3.1 Thermal reaction norms

The growth temperature curve (growth thermal norms) obtained for *E. huxleyi* (Fig. 1) exhibited different shapes for the LC and the HC-grown cells. The LC cultures showed an asymmetric pattern that is common to many algal species, in which the growth rate increased with rise in temperature to reach a maximum of 1.3 d^{-1} at 22.2 °C and then declined sharply at temperatures above this optimal point (Table 2). At 20 and 24 °C, the growth rate was < 10 % lower than at 22.2 °C; therefore, 20 and 24 °C were still within the optimal growth temperature range for LC-grown *E. huxleyi*. The HC-grown cells showed a relatively symmetric thermal norm, with an optimal growth temperature of 20.6 °C, 1.6 °C lower than that of the LC-grown cells. Thus the growth rate at 20 °C was near maximal, while the value at 24 °C decreased by nearly 20 % compared with the maximal growth rate. The net effect of these trends was that the growth rate of the LC-grown cells was significantly ($p < 0.05$) higher than that of the HC-grown cells at 22 and 24 °C (Fig. 1).

3.2 Growth rate

During the 10 generations of growth at two CO_2 levels and three temperatures prior to the UV exposure, the growth rate was lowest at 15 °C and was further reduced by 17.4 % in HC-grown cells compared with LC-grown cells ($p < 0.05$, Fig. 2). At 20 °C, there was no difference in growth rates between the HC- and LC-grown cells ($p > 0.05$). At 24 °C, the growth rate did not change in LC-grown cells ($p > 0.05$), but decreased in HC-grown cells compared to that at 20 °C;
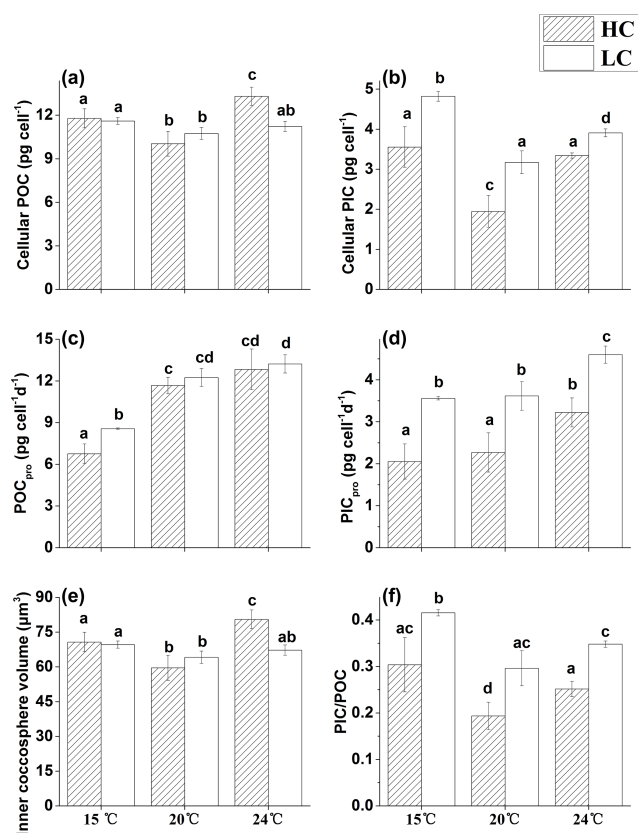
Figure 3. The cellular POC **(a)**, cellular PIC **(b)**, POC production rate **(c)**, PIC production rate **(d)**, inner coccosphere volume **(e)** and PIC / POC ratio **(f)** of *E. huxleyi* grown in 400 µatm (LC) and 1000 µatm (HC) CO_2 concentrations at 15, 20 and 24 °C, respectively. The different letters above the bars indicate significant differences among the treatments ($p < 0.05$). The values are the means, and the error bars are standard deviations for triplicate cultures for each treatment.
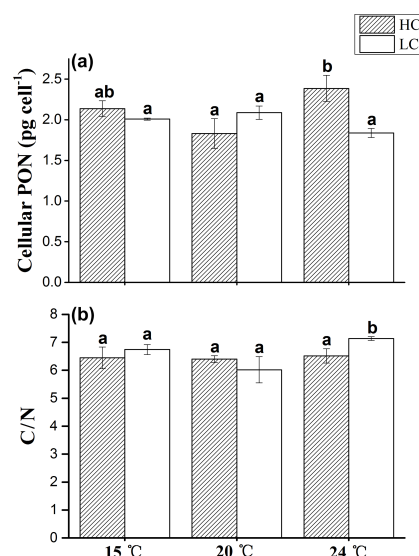

Figure 4. The cellular PON content **(a)** and C / N ratio **(b)** of *E. huxleyi* grown in 400 µatm (LC) and 1000 µatm (HC) CO_2 concentrations at 15, 20 and 24 °C, respectively. The different letters above the bars indicate significant differences among the treatments ($p < 0.05$). The values are the means, and the error bars are standard deviations for triplicate cultures for each treatment.

thus, the growth rate was 17.5 % lower in HC-grown cells compared with LC-grown cells at 24 °C ($p > 0.05$).

3.3 Cellular PIC and POC quotas, production rates and inner coccosphere volumes

The two CO_2 treatments had no effect on cellular POC content at 15 and 20 °C. However, at 24 °C, the HC treatment significantly increased cellular POC by 18.4 % compared with the LC treatment ($p < 0.01$, Fig. 3a), yielding the highest value among the treatments. Cellular PIC content was reduced with increased CO_2 concentration in the 15, 20 and 24 °C treatments by 35.8 % ($p < 0.05$, Fig. 3b), 62.6 % ($p < 0.05$) and 17.1 % ($p < 0.01$), respectively. In LC-grown cells, cellular PIC was significantly affected by temperature, with the highest values observed at 15 °C, a decrease of 34.2 % ($p < 0.01$) at 20 °C and a decrease 18.9 % ($p < 0.01$) at 24 °C. In HC-grown cells, cellular PIC was 45.2 % ($p < 0.01$) and 41.7 % ($p < 0.01$) lower at 20 °C, compared

with that at 15 and 24 °C, respectively. The production rate of POC ranged from 6.8 to 13.2 pg cell^{-1} d^{-1} among different treatments (Fig. 3c). At 15 °C, the HC treatment reduced the POC production rate by 26.6 % ($p < 0.05$), and the values were 42 % ($p < 0.01$) and 30 % ($p < 0.01$) lower in HC- and LC-grown cells, respectively, compared with those at 20 °C. No significant differences were observed between different CO_2 treatments at 20 and 24 °C ($p > 0.05$), and the temperature rising from 20 to 24 °C also had no significant effect on the POC production rate in either HC- or LC-grown cells ($p > 0.05$). The HC treatment lowered the PIC production rate by 42.3 % ($p < 0.01$, Fig. 3d), 37.3 % ($p < 0.01$) and 29.9 % ($p < 0.01$) at 15, 20 and 24 °C, respectively. A 5 °C temperature decrease from 20 °C had no significant effect on the PIC production rate in either the LC-cultures or the HC-cultures ($p > 0.05$). However, a 4 °C increase from 20 to 24 °C enhanced the PIC production rate by 41.9 % ($p < 0.05$) and 27.4 % ($p < 0.05$) in HC- and LC-grown cells, respectively.

The pattern of inner coccosphere volume among different treatments was similar to that of cellular POC (Fig. 3e), with a significantly higher value in HC-cultures than in LC-cultures at 24 °C ($p < 0.01$), while no difference existed between different CO_2 treatments at the other temperature levels ($p > 0.05$).

The PIC to POC ratio (PIC / POC) had the lowest value at 20 °C in the HC treatment (Fig. 3f), and the highest value at 15 °C in the LC treatment. Either reduced or elevated temper-
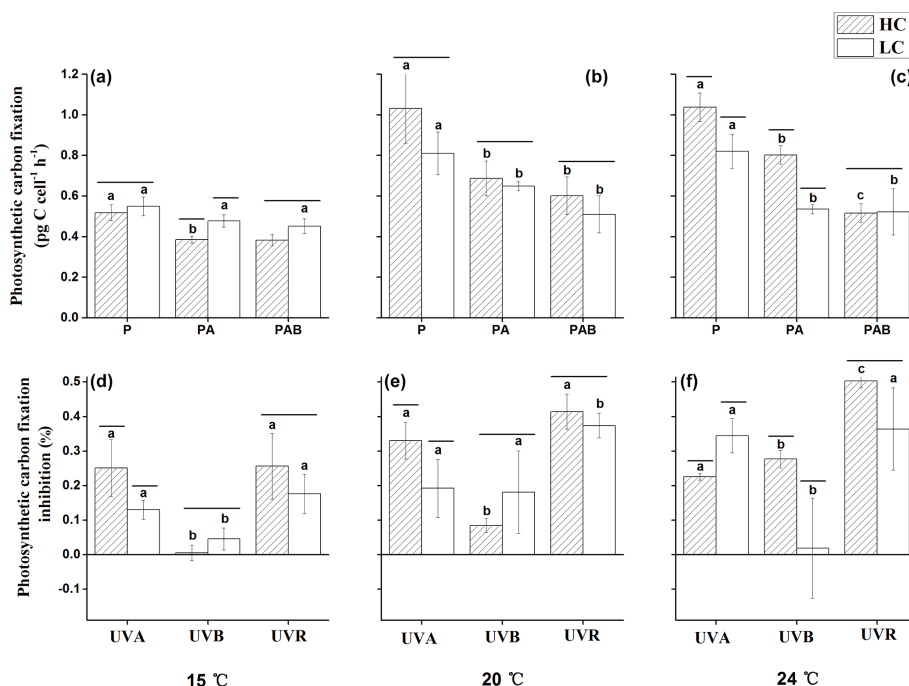
Figure 5. Photosynthetic carbon fixation rates **(a–c)** under P (irradiances above 395 nm), PA (irradiances above 320 nm) and PAB (irradiances above 295 nm), and inhibition of photosynthetic carbon fixation rates **(d–f)** due to UVA, UVB and UVR of *E. huxleyi* in HC- and LC-grown cells at 15, 20 and 25 °C . Lines above the histogram bars indicate significant differences between the HC and LC treatments, and the different letters indicate significant differences among the radiation treatments within the HC- or LC-grown cells within each panel.

ature from 20 °C increased the PIC / POC ratio in both HC- and LC-cultures ($p < 0.05$), although the extent varied.

3.4 Cellular PON content and POC / PON (C / N) ratio

Cellular PON displayed the same trends between the HC and LC treatments at 15 and 20 °C ($p > 0.05$, Fig. 4a). Similar to cellular POC, at 24 °C cellular PON was 29.6 % higher in HC-grown cells compared with LC-grown cells ($p < 0.01$).

The C / N ratio showed no significant difference among different temperatures in the HC treatment ($p > 0.05$, Fig. 4b). In the LC treatment, the C / N ratio was significantly higher at 24 °C than that at 15 and 20 °C ($p < 0.05$). The C / N ratio in the LC treatment was 9.5 % higher than that in the HC treatment at 24 °C ($p < 0.05$), while the value showed no significant difference between the HC and LC treatments at 15 and 20 °C ($p > 0.05$).

3.5 Responses of photosynthetic carbon fixation to UV radiation

After 3 h of exposure under the solar simulator, significant interactive effects between temperature and irradiance ($p < 0.01$), temperature and pCO_2 ($p < 0.01$), and irradiance and pCO_2 ($p = 0.042$) were observed on photosynthetic carbon fixation (Table 3). There were no differences in photosynthetic carbon fixation rates between HC- and LC-cultures at 15 °C under the PAR only treatment ($p > 0.05$, Fig. 5a),

while the values were marginally ($p = 0.064$, Fig. 5b) and significantly ($p = 0.026$, Fig. 5c) higher in HC-grown cells compared with LC-grown cells at 20 and 24 °C. At 15 °C, presence of UVA or UVR (UVA + UVB) had no significant effect on the photosynthetic rate under the LC conditions ($p > 0.05$); however, it lowered the photosynthetic rate under the HC conditions ($p < 0.01$, Fig. 5d). At 20 °C, the values were reduced by 33.4 % ($p < 0.05$) and 19.9 % ($p = 0.05$) in HC- and LC-grown cells under the PA treatment compared with the PAR only treatment (Fig. 5b, e). The PAB treatment did not further lower the photosynthetic rates compared to the PA treatment in either the HC- or LC-cultures ($p > 0.05$). At the highest temperature of 24 °C, the photosynthetic rate was 22.6 % ($p < 0.01$) and 34.8 % ($p < 0.01$) lower under the PA treatment compared to the PAR only treatment in HC- and LC-grown cells, respectively (Fig. 5c, f). The values were further decreased by 35.7 % ($p < 0.01$) in HC-grown cells, but were not affected in LC-grown cells in the PAB treatment ($p > 0.05$).

3.6 Calcification rates and Cal / Pho ratios in response to UV exposures

Calcification rates were significantly lower in HC-grown cells compared with LC-grown cells under the PAR only treatment at all temperature levels ($p < 0.01$, Fig. 6a–c). The PA treatment significantly increased the calcification rate in
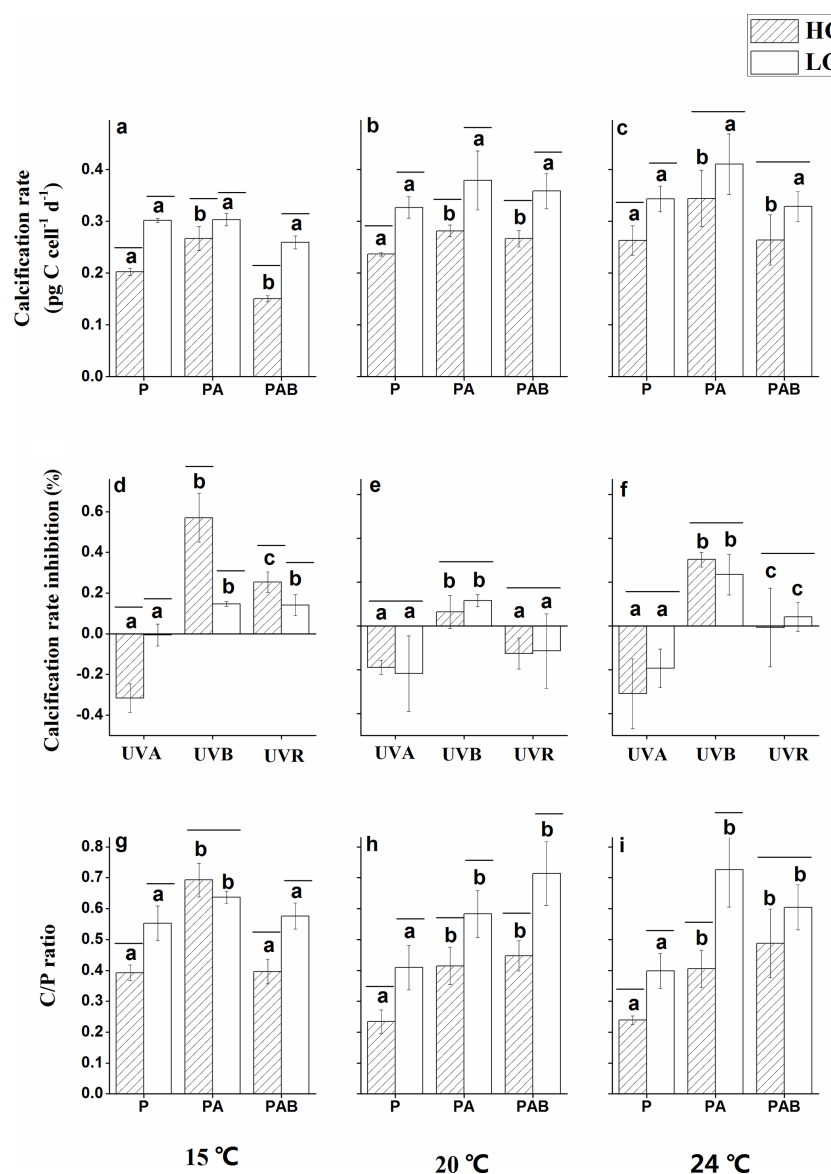
Figure 6. Calcification rates under P, PA and PAB **(a–c)**; inhibition of calcification rates due to UVA, UVB and UVR **(d–f)**; and Cal / Pho ratios under P, PA and PAB **(g–i)** for *E. huxleyi* in HC- and LC-grown cells at 15, 20 and 24 °C. Negative inhibition values indicate stimulation. Lines above the histogram bars indicate significant differences between the HC and LC treatments, and the different letters indicate significant differences among the radiation treatments within the HC or LC-grown cells within each panel.

HC-grown cells relative to the PAR only treatment by 31.7 % (Fig. 6a, d), 18.9 % (Fig. 6b, e) and 30.3 % (Fig. 6c, f) at 15, 20 and 24 °C, respectively ($p < 0.05$). However, there were no significant differences in calcification rates between PA and PAR treatments in LC-grown cells ($p > 0.05$). Under the PAB treatment, the presence of UVB led to a reduced calcification rate compared with the PA treatment at 15 °C ($p < 0.01$). This inhibition was significantly higher in HC-cultures compared to LC-cultures (Fig. 6a, d), but there were no significant differences in the calcification rates between the PA and PAB treatments at 20 and 24 °C ($p > 0.05$) in either HC- or LC-grown cells. There were significant interac-

tions between temperature and irradiance on the calcification rate ($p = 0.018$).

The calcification to photosynthesis ratio (Cal / Pho ratio) values were significantly higher under PA than in the PAR only treatment ($p < 0.05$, Fig. 6g–i), regardless of the CO_2 concentrations and temperature levels. The Cal / Pho ratio was lower at 15 °C under PAB compared with the PA treatment in both HC-grown ($p < 0.01$) and LC-grown ($p < 0.05$) cells, while there were no significant differences between these irradiance treatments at 20 and 24 °C ($p > 0.05$). Except in the PA treatment at 15 °C, the Cal / Pho ratio was significantly lower in HC-grown cells compared with LC-

Table 1. Mean values of the seawater carbonate system parameters under HC (1000 µatm) and LC (400 µatm) at 15, 20 and 24 °C. The cell concentrations of all cultures were maintained below 5×10^4 cells mL^{-1} and pH variations were < 0.04 units.

	Treatment	pH$_{NBS}$	DIC (µmol kg^{-1})	pCO$_2$ (µatm)	HCO$_3^-$ (µmol kg^{-1})	CO$_3^{2-}$ (µmol kg^{-1})	Total alkalinity (µmol kg^{-1})
15 °C	HC	7.80 ± 0.02[a]	2147.2 ± 105.7[a]	1000 ± 40[a]	2037.5 ± 98.6[a]	72.4 ± 7[a]	2228.5 ± 114.4[a]
	LC	8.13 ± 0.01[b]	1919.2 ± 27.2[b]	400 ± 40[b]	1768.1 ± 23.6[b]	136.2 ± 3.6[b]	2122.8 ± 31.7[a]
20 °C	HC	7.82 ± 0.01[a]	2153.2 ± 57.3[a]	1000 ± 40[a]	2031.5 ± 52.8[a]	89.74 ± 4.5[a]	2262.7 ± 62.9[a]
	LC	8.16 ± 0.01[b]	1961.8 ± 25.7[b]	400 ± 40[b]	1777.8 ± 21.8[b]	170.13 ± 3.9[b]	2214.38 ± 30.4[a]
25 °C	HC	7.84 ± 0.01[a]	2057.2 ± 28.1[a]	1000 ± 40[a]	2174.8 ± 26.2[a]	106.3 ± 2.5[a]	2310.3 ± 31.2[a]
	LC	8.18 ± 0.01[b]	1854.6 ± 46.5[b]	400 ± 40[b]	1999.8 ± 38.4[b]	203.1 ± 8.2[b]	2297.2 ± 56.4[a]

The superscripts letters represent a significant difference between HC and LC ($p < 0.05$).

Table 2. The optimal temperature for growth (T_{opt}) and the maximum growth rate (μ_{max}) at T_{opt} for *E. huxleyi* grown in 400 µatm (LC) and 1000 µatm (HC) CO$_2$ concentrations. T_{opt} and μ_{max} as estimated from the fitted curves in Fig. 1 by numerical optimization.

	T_{opt} (°C)	μ_{max} (μ)
HC	20.58	1.22
LC	22.15	1.31

grown cells under all of the other conditions, with the greatest reduction of 44.3 % at 24 °C. There were significant interactions among all three variables for the Cal / Pho ratio ($p < 0.01$).

4 Discussion

Our results demonstrated that both photosynthesis and calcification were inhibited by UVB. In contrast, UVA was more inhibitory for photosynthesis than UVB, while it had a positive effect on calcification. The degree to which UVA and UVB affected the performance of photosynthesis and calcification varied depending on CO$_2$ concentrations and temperature levels. Of the three temperature levels used, 15 °C was much lower than the optimal growth temperature for both HC- and LC- grown cells. For LC cultures, the growth rate was the same at 20 and 24 °C, and these two temperatures were in the optimal range for cell growth. While 20 °C was very close to the optimal temperature for HC-grown cells, the growth rate at 24 °C was significantly reduced, suggesting that the cell growth at this temperature may already be thermally inhibited. The different growth state among the three temperature levels, particularly that between HC- and LC-grown cells at the highest temperature, potentially affected the photosynthetic and calcification responses to UV radiation.

In this study, the inhibition of photosynthesis by UVA, UVB and their combination appeared to increase with temperature. On the contrary, previous studies conducted on other phytoplankton species such as diatoms have suggested that increasing temperature could reduce UV-induced inhibition of photosynthesis, as the activities of repair-associated enzymes are temperature dependent (Li et al., 2012; Helbling et al., 2011). These differing trends between the present work and previous studies may be attributed to either changes in the thickness of the coccolith layer surrounding the cells, or to the temperature range used. The coccoliths of *E. huxleyi* can play a protective role against UVR by either strongly scattering light, or by physically shading intracellular organelles (Xu et al., 2016; Voss et al., 1998). In our results, the cellular PIC at 20 °C was only half of that at 15 °C. As cellular PIC is an indicator of the amount of coccoliths on the exterior of the cell, this suggests that the cells grown at 20 °C had a substantially thinner coccolith layer and consequently received much more UV radiation, leading to increased photosynthetic damage compared with cells grown at 15 °C. At 24 °C, the thermal reaction curves suggested that this temperature level was already close to the upper tolerance limit for growth in *E. huxleyi* PML B92/11, with HC-grown cells suffering more thermal stress. At this temperature, although the thickness of the coccolith layer was equal to that at 15 °C, biochemical aspects of UVR defense and/or repair mechanisms may be under thermal stress (Sobrino and Neale, 2007).

At 15 and 20 °C the inhibition of photosynthesis was mainly caused by UVA, and the values were significantly higher in HC-grown cells compared with LC-grown cells, due to a thinner coccolith layer on cells in acidified seawater (Gao et al., 2009). In contrast, at 24 °C the HC treatment alleviated the UVA-induced inhibition compared with the LC treatment but also greatly enhanced inhibition by UVB. The underlying mechanism may be protein-mediated defense/repair processes. This is supported by the fact that the C / N ratio was only increased by the LC treatment at 24 °C. The C / N ratio can reflect the defense and repair ability of

Table 3. Three-way ANOVA analyses of interactive effects among $p\text{CO}_2$ (CO_2), temperature (T) and irradiance (I, including P, PA and PAB) on photosynthetic carbon fixation rates, calcification rates and Cal / Pho ratios, respectively. Also shown are three-way ANOVA analyses of interactive effects among CO_2 (CO_2), temperature (T) and irradiance (I, including UVA, UVB and UVR) on the inhibition (Inh) of photosynthesis (Pho), calcification (Cal) and the Cal / Pho ratios, respectively.

	$T \times I$ $p\,(\mathrm{d}f, F)$	$T \times \text{CO}_2$ $p\,(\mathrm{d}f, F)$	$I \times \text{CO}_2$ $p\,(\mathrm{d}f, F)$	$T \times I \times \text{CO}_2$ $p\,(\mathrm{d}f, F)$
Pho rate	$< 0.01^{**}$ $(4, 7.220)$	$< 0.01^{**}$ $(2, 11.505)$	0.042^{*} $(2, 3.453)$	0.055 $(4, 2.560)$
Cal rate	0.018^{*} $(4, 3.432)$	0.541 $(2, 0.625)$	0.465 $(2, 0.783)$	0.483 $(4, 0.885)$
Cal / Pho ratio	$< 0.01^{**}$ $(4, 8.253)$	0.03^{*} $(2, 3.874)$	0.632 $(2, 0.464)$	0.002^{**} $(4, 5.155)$
Inh of Pho rate	0.231 $(4, 1.473)$	0.381 $(2, 0.991)$	0.565 $(2, 0.580)$	$< 0.01^{**}$ $(4, 8.546)$
Inh of Cal rate	0.01^{**} $(4, 3.928)$	0.24 $(2, 1.484)$	$< 0.01^{**}$ $(2, 8.881)$	$< 0.01^{**}$ $(4, 6.610)$
Inh of Cal / Pho ratio	0.021^{*} $(4, 3.331)$	0.108 $(2, 2.365)$	0.127 $(2, 2.186)$	$< 0.01^{**}$ $(4, 6.727)$

* and ** represent significance levels at $p < 0.05$ and 0.01, respectively.

cells against UVR (Sobrino et al., 2008; Litchman et al., 2002). Phytoplankton use several mechanisms to repair UV-induced damage, many of which involve nitrogen-requiring enzymes and/or protein cofactors (Litchman et al., 2002). Korbee et al. (2010) reported that UVA could stimulate algae nitrogen metabolism (nitrate transport and reductase activity). In contrast, UVB was found to damage cell membranes and negatively affect nitrogen incorporation mechanisms, leading to an increase in the C / N ratio (Sobrino et al., 2004). Such a lack of nitrogen would subsequently inhibit essential protein turnover. In our study at 24 °C, UVA and HC might act synergistically to maintain a lower C / N ratio and support the synthesis of UV-repair proteins, thereby partially counteracting the UV-induced damage. As mentioned above, at 24 °C HC-grown cells were already thermally inhibited, which may add the detrimental effect of UVB on nitrogen assimilation and lead to a much higher inhibition of photosynthesis by UVB in high CO_2, warmer conditions.

When assessing the effect of UV radiation on calcification, we found that UVA stimulated the calcification rate of *E. huxleyi* PML B92/11, while UVB inhibited it. In earlier studies, Gao et al. (2009) reported that both UVA and UVB negatively affected the calcification of *E. huxleyi* CS-369. One possibility for this discrepancy between our studies can be attributed to strain-specific responses. Conversely, the different irradiances used by the two studies could also be involved, as the light intensity utilized by Gao et al. (2009) was over twice as high as the one we used. Similarly to our study, Xu and Gao (2015) also observed that moderate levels of UVR increased PIC production rates. It has been demonstrated that

E. huxleyi can use only bicarbonate to support its calcification (Kottmeier et al., 2016; Paasche, 2002). Thus, the observed stimulation of calcification by UVA can perhaps be attributed to UVA-enhanced bicarbonate utilization (Xu and Gao, 2010).

Given that the responses of coccolithophore strains to environmental change can be different depending on the strain's temperature optimum (Sett et al., 2014), the temperatures we chose in this study were below, close to or above optimum for *E. huxleyi* growth based on its thermal tolerance curves. The lower temperature of 15 °C that we used was around the mean summer surface water temperature in the region where *E. huxleyi* PML B92/11 was isolated (Fielding, 2013). A temperature of 20 °C, in comparison, represents a future warmer condition, with 24 °C likely being similar to the upper limit of temperatures that will be experienced by this strain due to temperature fluctuations in the future. In the present study, we found that UV radiation could interact with both temperature and CO_2 concentration to alter their effects on photosynthesis and calcification, thus changing Cal / Pho ratios. The interactive effects of elevated CO_2 and UV radiation on non-calcifying marine organism have been extensively reported (Li et al., 2012; Gao et al., 2012). With regard to the calcifying coccolithophore *E. huxleyi*, OA generally reduces their calcification (thinner coccolith layer) as well as the Cal / Pho ratio, based on a number of indoor laboratory experiments with UV-free light sources (Tong et al., 2018). In the present study, with increasing temperature, we found that there was no significant difference in the Cal / Pho ratios between high and low CO_2-grown cells under UV radiation

at 24 °C. The light intensity used was equivalent to the mean light level in the upper mixed layer (UML) based on time series station (19° N, 118.5° E) measurements in the South China Sea. Our results imply that *E. huxleyi* exposed to moderate levels of solar radiation can sustain their cell density with a constant Cal / Pho ratio under progressive warming and acidification. However, considering the slow mixing of the upper layer during the daytime, cells dwelling in a shallower UML are likely to be exposed to higher doses of solar irradiances. Under such circumstances, UV radiation is most likely to reduce Cal / Pho ratios in *E. huxleyi*, and ocean acidification will exacerbate the effect of UV radiation (Gao et al., 2009). As a result, the net effects of temperature, CO_2 concentration and UV radiation will largely depend on the levels of solar radiation to which the cells are exposed.

In previous studies, most indoor laboratory experiments neglected the effects of UV radiation due to the common use of UV-free light sources or UV-opaque vessels. Our results demonstrated that UV radiation could greatly influence the combined effects of future CO_2 enrichment and sea surface warming on the physiological performance of *E. huxleyi*. Thus, the impacts UV radiation should be considered in order to build more realistic predictions of future biological and biogeochemical processes in a high-CO_2 ocean.

References

Alexiadis, A.: Global warming and human activity: A model for studying the potential instability of the carbon diox-ide/temperature feedback mechanism, Ecol. Model., 203, 243–256, doi:10.1016/j.ecolmodel.2006.11.020, 2007.

Cai, W.-J., Hu, X., Huang, W.-J., Murrell, M. C., Lehrter, J. C., Lohrenz, S. E., Chou, W.-C., Zhai, W., Hollibaugh, J. T., and Wang, Y.: Acidification of subsurface coastal waters enhanced by eutrophication, Nat. Geosci., 4, 766–770, https://doi.org/10.1038/ngeo1297, 2011.

Chen, C.-C., Shiah, F.-K., Chung, S.-W., and Liu, K.-K.: Winter phytoplankton blooms in the shallow mixed layer of the South China Sea enhanced by upwelling, J. Mar. Syst., 59, 97–110, https://doi.org/10.1016/j.jmarsys.2005.09.002, 2006.

Dickson, A. G.: Standard potential of the reaction: AgCl(s) + 12H$_2$(g)=Ag(s) + HCl(aq), and the standard acidity constant of the ion HSO$_4^-$ in synthetic sea water from 273.15 to 318.15 K, J. Chem. Thermodyn., 22, 113–127, https://doi.org/10.1016/0021-9614(90)90074-Z, 1990.

Feng, Y., Warner, M. E., Zhang, Y., Sun, J., Fu, F.-X., Rose, J., and Hutchins, D. A.: Interactive effects of increased pCO_2, temperature and irradiance on the marine coccolithophore *Emiliania huxleyi* (Prymnesiophyceae), Eur. J. Phycol., 43, 87–98, https://doi.org/10.1080/09670260701664674, 2008.

Fielding, S. R.: *Emiliania huxleyi* specific growth rate dependence on temperature, Limnol. Oceanogr., 58, 663–666, https://doi.org/10.4319/lo.2013.58.2.0663, 2013.

Gao, K., Wu, Y., Li, G., Wu, H., Villafañe, V. E., and Helbling, E. W.: Solar UV Radiation Drives CO_2 Fixation in Marine Phytoplankton: A Double-Edged Sword, Plant Physiol., 144, 54–59, https://doi.org/10.1104/pp.107.098491, 2007.

Gao, K., Ruan, Z., Villafan, V. E., Gattuso, J.-P., and Helbling, E. W.: Ocean acidification exacerbates the effect of UV radiation on the calcifying phytoplankter *Emiliania huxleyi*, Limnol. Oceanogr., 54, 1855–1862, https://doi.org/10.4319/lo.2009.54.6.1855 2009.

Gao, K., Helbling, E. W., Häder, D.-P., and Hutchins, D. A.: Responses of marine primary producers to interactions between ocean acidification, solar radiation, and warming, Mar. Ecol. Prog. Ser., 470, 167–189, https://doi.org/10.3354/meps10043, 2012.

Gattuso, J.-P., Pichon, M., and Frankignoulle, M.: Biological control of air-sea CO_2 fluxes: effect of photosynthetic and calcifying marine organisms and ecosystems, Oceanogr. Lit. Rev., 7, 663–664, https://doi.org/10.3354/meps129307, 1996.

Gattuso, J.-P., Magnan, A., Billé, R., Cheung, W. W. L., Howes, E. L., Joos, F., Allemand, D., Bopp, L., Cooley, S. R., Eakin, C. M., Hoegh-Guldberg, O., Kelly, R. P., Pörtner, H.-O., Rogers, A. D., Baxter, J. M., Laffoley, D., Osborn, D., Rankovic, A., Rochette, J., Sumaila, U. R., Treyer, S., and Turley, C.: Contrasting futures for ocean and society from different anthropogenic CO_2 emissions scenarios, Science, 349, aac4722, https://doi.org/10.1126/science.aac4722, 2015.

Guan, W. and Gao, K.: Impacts of UV radiation on photosynthesis and growth of the coccolithophore *Emiliania huxleyi* (Haptophyceae), Environ. Exp. Bot., 67, 502–508, https://doi.org/10.1016/j.envexpbot.2009.08.003, 2009.

Häder, D.-P. and Gao, K.: Interactions of anthropogenic stress factors on marine phytoplankton, Front. Environ. Sci., 3, 1–14, https://doi.org/10.3389/fenvs.2015.00014, 2015.

Häder, D.-P., Williamson, C. E., Wängberg, S.-Å., Rautio, M., Rose, K. C., Gao, K., Helbling, E. W., Sinhah, R. P., and Worrest, R.:

Effects of UV radiation on aquatic ecosystems and nteractions with other environmental factors, Photoch. Photobio. Sci., 10, 113–150, https://doi.org/10.1039/c4pp90035a, 2014.

Helbling, E. W., Gao, K., Gonçalves, R. J., Wu, H., and Villafañe, V. E.: Utilization of solar UV radiation by coastal phytoplankton assemblages off SE China when exposed to fast mixing, Mar. Ecol. Prog. Ser., 259, 59–66, https://doi.org/10.3354/meps259059, 2003.

Helbling, E. W., Buma, A. G. J., Boelen, P., van der Strate, H. J., Giordanino, M. V. F., and Villafañe, V. E.: Increase in Rubisco activity and gene expression due to elevated temperature partially counteracts ultraviolet radiation-induced photoinhibition in the marine diatom *Thalassiosira weissflogii*, Limnol. Oceanogr., 56, 1330–1342, https://doi.org/10.4319/lo.2011.56.4.1330, 2011.

Hutchins, D. A. and Fu, F.: Microorganisms and ocean global change, Nat. Microbiol., 2, 17058, https://doi.org/10.1038/nmicrobiol.2017.58, 2017.

Jin, P., Ding, J., Xing, T., Riebesell, U., and Gao, K.: High levels of solar radiation offset impacts of ocean acidification on calcifying and non-calcifying strains of *Emiliania huxleyi*, Mar. Ecol. Prog. Ser., 568, 47–58, https://doi.org/10.3354/meps12042 2017.

Korbee, N., Mata, M. T., and Figueroa, F. l. L.: Photoprotection mechanisms against ultraviolet radiation in *Heterocapsa* sp. (Dinophyceae) are influenced by nitrogen availability: Mycosporine-like amino acids vs. xanthophyll cycle, Limnol. Oceanogr., 55, 899–908, https://doi.org/10.4319/lo.2010.55.2.0899, 2010.

Kottmeier, D. M., Rokitta, S. D., and Rost, B.: Acidification, not carbonation, is the major regulator of carbon fluxes in the coccolithophore *Emiliania huxleyi*, New Phytol., 211, 126–137, https://doi.org/10.1111/nph.13885, 2016.

Langer, G., Nehrke, G., Probert, I., Ly, J., and Ziveri, P.: Strain-specific responses of *Emiliania huxleyi* to changing seawater carbonate chemistry, Biogeosciences, 6, 2637–2646, https://doi.org/10.5194/bg-6-2637-2009, 2009.

Lewis, E., Wallace, D., and Allison, L. J.: Program developed for CO_2 system calculations, Carbon Dioxide Information Analysis Center, managed by Lockheed Martin Energy Research Corporation for the US Department of Energy Tennessee, 1998.

Li, Y., Gao, K., Villafañe, V. E., and Helbling, E. W.: Ocean acidification mediates photosynthetic response to UV radiation and temperature increase in the diatom *Phaeodactylum tricornutum*, Biogeosciences, 9, 3931–3942, https://doi.org/10.5194/bg-9-3931-2012, 2012.

Litchman, E., Neale, P. J., and Banaszak, A. T.: Increased sensitivity to ultraviolet radiation in nitrogen-limited dinoflagellates: Photoprotection and repair, Limnol. Oceanogr., 47, 86–94, https://doi.org/10.4319/lo.2002.47.1.0086, 2002.

Menden-Deuer, S. and Lessard, E. J.: Carbon to volume relationships for dinoflagellates, diatoms, and other protist plankton, Limnol. Oceanogr., 45, 569–579, https://doi.org/10.4319/lo.2000.45.3.0569, 2000.

Milner, S., Langer, G., Grelaud, M., and Ziveri, P.: Ocean warming modulates the effects of acidification on *Emiliania huxleyi* calcification and sinking, Limnol. Oceanogr., 61, 1322–1336, 2016.

Monteiro, F. M., Bach, L. T., Brownlee, C., Bown, P., Rickaby, R. E., Poulton, A. J., Tyrrell, T., Beaufort, L., Dutkiewicz, S., and Gibbs, S.: Why marine phytoplankton calcify, Sci. Adv., 2, e1501822, https://doi.org/10.1126/sciadv.1501822, 2016.

Norberg, J.: Biodiversity and ecosystem functioning: A complex adaptive systems approach, Limnol. Oceanogr., 49, 1269–1277, https://doi.org/10.4319/lo.2004.49.4_part_2.1269, 2004.

Paasche, E.: The effect of temperature, light intensity, and photoperiod on coccolith formation, Limnol. Oceanogr., 13, 178–181, https://doi.org/10.4319/lo.1968.13.1.0178, 1968.

Paasche, E.: A review of the coccolithophorid *Emiliania huxleyi* (Prymnesiophyceae), with particular reference to growth, coccolith formation, and calcification-photosynthesis interactions, Phycologia, 40, 503–529, https://doi.org/10.2216/i0031-8884-40-6-503.1, 2002.

Raitsos, D. E., Lavender, S. J., Pradhan, Y., Tyrrell, T., Reid, P. C., and Edwards, M.: Coccolithophore bloom size variation in response to the regional environment of the subarctic North Atlantic, Limnol. Oceanogr., 51, 2122–2130, https://doi.org/10.4319/lo.2006.51.5.2122, 2006.

Raven, J. A. and Crawfurd, K.: Environmental controls on coccolithophore calcification, Mar. Ecol. Prog. Ser., 470, 137–166, https://doi.org/10.3354/meps09993, 2012.

Riebesell, U., Zondervan, I., Rost, B., Tortell, P. D., Zeebe, R. E., and Morel, F. M. M.: Reduced calcification of marine plankton in response to increased atmospheric CO_2, Nature, 407, 364–367, https://doi.org/10.1038/35030078, 2000.

Riebesell, U., Bach, L. T., Bellerby, R. G. J., Monsalve, J. R. B., Boxhammer, T., Czerny, J., Larsen, A., Ludwig, A., and Schulz, K. G.: Competitive fitness of a predominant pelagic calcifier impaired by ocean acidification, Nat. Geosci., 10, 19–24, https://doi.org/10.1038/NGEO2854, 2017.

Rost, B. and Riebesell, U.: Coccolithophores and the biological pump: responses to environmental changes, in: Coccolithophores, Springer, 99–125, 2004.

Roy, R. N., Roy, L. N., Vogel, K. M., Porter-Moore, C., Pearson, T., Good, C. E., Millero, F. J., and Campbell, D. M.: The dissociation constants of carbonic acid in seawater at salinities 5 to 45 and temperatures 0 to 45 °C, Mar. Chem., 44, 249–267, 1993.

Sett, S., Bach, L. T., Schulz, K. G., Koch-Klavsen, S., Lebrato, M., and Riebesell, U.: Temperature modulates coccolithophorid sensitivity of growth, photosynthesis and calcification to increasing seawater pCO_2, Plos One, 9, 1–9, https://doi.org/10.1371/journal.pone.0088308, 2014.

Sobrino, C. and Neale, P. J.: Short-term and long-term effects of temperature on photosynthesis in the diatom *Thalassiosira Pseudonana* under UVR exposures, J. Phycol., 43, 426–436, https://doi.org/10.1111/j.1529-8817.2007.00344.x, 2007.

Sobrino, C., Montero, O., and Lubián, L. M.: UV-B radiation increases cell permeability and damages nitrogen incorporation mechanisms in *Nannochloropsis gaditana*, Aquat. Sci., 66, 421–429, https://doi.org/10.1007/s00027-004-0731-8, 2004.

Sobrino, C., Ward, M. L., and Neale, P. J.: Acclimation to elevated carbon dioxide and ultraviolet radiation in the diatom *Thalassiosira pseudonana*: Effects on growth, photosynthesis, and spectral sensitivity of photoinhibition, Limnol. Oceanogr., 53, 494–505, https://doi.org/10.4319/lo.2008.53.2.0494, 2008.

Stocker, T., Qin, D., Plattner, G.-K., Tignor, M., Allen, S. K., Boschung, J., Nauels, A., Xia, Y., Bex, V., and Midgley, P. M.: Climate Change 2013: The physical science basis, Cambridge University Press Cambridge, UK, New York, USA, 2014.

Sunda, W. G., Price, N. M., and Morel, F. M.: Trace metal ion buffers and their use in culture studies, Algal Culturing Techniques, 4, 35–63, 2005.

Tedetti, M., Sempéré, R., Vasilkov, A., Charriere, B., Nérini, D., Miller, W. L., Kawamura, K., and Raimbault, P.: High penetration of ultraviolet radiation in the south east Pacific waters, Geophys. Res. Lett., 34, L12610, https://doi.org/10.1029/2007GL029823, 2007.

Thomas, M. K., Kremer, C. T., Klausmeier, C. A., and Litchman, E.: A Global Pattern of Thermal Adaptation in Marine Phytoplankton, Science, 338, 1085–1088, https://doi.org/10.1126/science.1224836, 2012.

Tong, S., Hutchins, D. A., Fu, F., and Gao, K.: Effects of varying growth irradiance and nitrogen sources on calcification and physiological performance of the coccolithophore *Gephyrocapsa oceanica* grown under nitrogen limitation, Limnol. Oceanogr., 61, 2234–2242, https://doi.org/10.1002/lno.10371, 2016.

Tong, S., Gao, K., and Hutchins, D. A.: Adaptive evolution in the coccolithophore *Gephyrocapsa oceanica* following 1,000 generations of selection under elevated CO_2, Global Change Biol., 24, 3055–3064, https://doi.org/10.1111/gcb.14065, 2018.

Voss, K. J., Balch, W. M., and Kilpatrick, K. A.: Scattering and attenuation properties of Emiliania Huxleyi cells and their detached coccoliths, Limnol. Oceanogr., 43, 870–876, https://doi.org/10.4319/lo.1998.43.5.0870, 1998.

Williamson, C. E., Zepp, R. G., Lucas, R. M., Madronich, S., Austin, A. T., Ballaré, C. L., Norval, M., Sulzberger, B., Bais, A. F., McKenzie, R. L., Robinson, S. A., Häder, D.-P., Paul, N. D., and Bornman, J. F.: Solar ultraviolet radiation in a changing climate, Nat. Clim. Change, 4, 434–441, https://doi.org/10.1038/nclimate2225, 2014.

Wu, Y., Gao, K., Li, G., and Helbling, E. W.: Seasonal Impacts of Solar UV Radiation on Photosynthesis of Phytoplankton Assemblages in the Coastal Waters of the South China Sea, Photochem. Photobiol., 86, 586–592, https://doi.org/10.1111/j.1751-1097.2009.00694.x, 2010.

Xu, J. and Gao, K.: Use of UV-A Energy for Photosynthesis in the Red Macroalga *Gracilaria lemaneiformis*, Photochem. Photobiol., 86, 580–585, https://doi.org/10.1111/j.1751-1097.2010.00709.x, 2010.

Xu, J., Bach, L. T., Schulz, K. G., Zhao, W., Gao, K., and Riebesell, U.: The role of coccoliths in protecting *Emiliania huxleyi* against stressful light and UV radiation, Biogeosciences, 13, 4637–4643, https://doi.org/10.5194/bg-13-4637-2016, 2016.

Xu, K. and Gao, K.: Solar UV Irradiances Modulate Effects of Ocean Acidification on the Coccolithophorid *Emiliania huxleyi*, Photochem. Photobiol., 91, 92–101, https://doi.org/10.1111/php.12363, 2015.